International Journal of Thermal Sciences 48 (2009) 1523–1529

Contents lists available at ScienceDirect

International Journal of Thermal Sciences

www.elsevier.com/locate/ijts

Linear stability analysis of the steady thermal regimes of a packed bed reactor with an organized structure

Eugen Magyari

Institut für Hochbautechnik, ETH-Zürich, Wolfgang-Pauli_Str. 1, CH-8093 Zürich, Switzerland

ARTICLE INFO

Article history:
Received 10 September 2008
Received in revised form 12 December 2008
Accepted 16 December 2008
Available online 9 January 2009

Keywords:
Exothermic reaction
Packed bed
Organized structure
Steady states
Dual solutions
Linear stability
Marginal stability

ABSTRACT

The linear stability of steady temperature distributions in a parallel-plane packed bed reactor is investigated analytically and numerically. A plane-parallel stratification of the reactive granular material is assumed which modulates the rate of the local volumetric heat generation by exothermic reactions. The approach is based on an exactly solvable nonlinear model which involves two experimentally accessible control parameters, the *intensity parameter* $\lambda > 0$ and *stratification parameter* $s \geqslant 0$. For a given value of s, an upper bound $\lambda_{\max}(s)$ of λ exists, such that above of this maximum the reactor becomes thermally uncontrollable. Below $\lambda_{\max}(s)$, unique as well as dual solutions exist. The former ones describe high temperature steady states of the reactor, while the dual solution branches are associated with low and high temperature reaction regimes, respectively. It is found that the low temperature branch is always linearly stable and the upper one unstable. The steady state of the reactor corresponding to the matching point $\lambda = \lambda_{\max}(s)$ of the low- and high-temperature solutions is marginally stable for all $s \geqslant 0$.

1. Introduction

The aim of the present paper is the linear stability analysis of the possible steady temperature distributions of the parallel-plane packed bed reactor described recently in [1]. The reactor considered in [1] is characterized by a *stratified structure* in the transversal direction and by the presence of *volumetric heat generation* by exothermic reactions. A special attention has been given in [1] to the occurrence of hot spots [2] and to the upper bounds of the existence domain of steady solutions [3], which represent in such processes the regime above of which the reactor becomes uncontrollable and thermal explosion may occur. The model calculations reported in [1] (and summarized in Section 2 below) apply to reactors encountered in the chemical process engineering, in civil engineering, combustion engineering, thermal explosion control and environmental energy engineering. Specific examples in these fields are the ethanol production from cereals in anaerobic fermenters (see e.g. [4]), hardening of the cement paste of massive concrete members, [5–8], burning of granular fuels, thermal explosion o fine powders (see e.g. [9]), degradation of organic waste materials in aerobic reactors and natural landfills, etc.

2. Basic equations and steady state solutions

In paper [1] a packed bed reactor with parallel plane boundaries kept at constant temperatures $T_1 = T_2 \equiv T_0$ was considered. The x-axis of the coordinate system was chosen perpendicular to the boundaries located at $x = -L$ and $x = +L$, such that the boundary conditions are $T|_{x=-L} = T|_{x=+L} = T_0$. The reactor is filled with a mixture of a fine granular material of which chemical composition varies with the x-coordinate continuously. There has been assumed that in this *organized structure* an exothermic chemical or biochemical reaction occurs, such that the rate of the volumetric heat generation is a continuous function both of the local temperature T and the coordinate x. The temperature field $T = T(x,t)$ in this parallel plane reactor is governed by the Fourier equation

$$\rho c \frac{\partial T}{\partial t} = k \frac{\partial^2 T}{\partial x^2} + Q(x,T) \tag{1}$$

where $Q(x,t)$ is the rate of volumetric heat generation by the exothermic reaction, being given by the Arrhenius law

$$Q(x,T) = Q_0(x) e^{-E_a/(k_B T)} \tag{2}$$

where $E_a > 0$ is the activation energy of the reaction and k_B the Boltzmann constant. The density ρ, the specific heat c and the thermal conductivity k of the material are slowly varying functions of the coordinate x and of reaction time t, such that all of them may be considered as constants. Using the leading-order Frank–Kamenetskii expansion of the Arrhenius exponential around $T - T_0$, [10], and introducing the dimensionless variables

$$X = \frac{x}{L}, \qquad \tau = \frac{t}{t_0}, \qquad \theta(X,\tau) = \alpha(T - T_0)$$
$$\Lambda(X) = (\alpha L^2/k) e^{-\alpha T_0} Q_0(x) \tag{3}$$

E-mail addresses: magyari@hbt.arch.ethz.ch, magyari@bluewin.ch.

1290-0729/$ – see front matter
doi:10.1016/j.ijthermalsci.2008.12.005

Nomenclature

c	specific heat ..... J/kg K
$C_{\rm I}$, $C_{\rm II}$	coefficients of linear combinations
E_a	activation energy ..... J
k	thermal conductivity ..... W/m K
k_B	Boltzmann constant ..... 1.38×10^{-23} J/K
K	integration constant
K_*	threshold value e^s of K
$\tilde{K}_*$	dual counterpart of K
L	half-thickness of packed bed ..... m
$P_\nu^\mu(z)$	associated Legendre functions of first kind
$Q_\nu^\mu(z)$	associated Legendre functions of second kind
q	dimensionless wall heat flux
Q	rate of volumetric heat generation ..... W/m^3
$Q_{\rm tot}$	dimensionless rate of local heat release
s	stratification parameter
t	time variable ..... s
t_0	time unit, $t_0=\rho cL^2/k$ ..... s
T	absolute temperature ..... K
T_0	boundary temperature ..... K
x	dimensional transversal coordinate ..... m
X	dimensionless transversal coordinate, $X=x/L$
X_0	integration constant
V	analogous Schrödinger potential
W	dimensionless function, $W=\theta+sX$
z	dimensionless variable, $z=\tanh\xi$

Greek symbols

α	constant, $\alpha=E_a/(k_BT_0^2)$ ..... K^{-1}
ε	rescaled eigenvalues, $\varepsilon=2\bar{\varepsilon}/(\lambda K)$
$\bar{\varepsilon}$	eigenvalues
φ	eigenfunctions
$\bar{\varphi}$	normalized eigenfunctions
λ	intensity parameter
Λ	dimensionless structure function of stratification, $\Lambda=\lambda e^{sX}$
μ	parameter, $\mu=\sqrt{-\varepsilon}=i\sqrt{\varepsilon}$
ρ	density ..... kg/m^3
θ	dimensionless temperature, $\theta=\alpha(T-T_0)$
τ	dimensionless time, $\tau=t/t_0$
ξ	dimensionless variable, Eq. (17)

Subscripts

max	related to maximum value of λ
n	order of eigenvalues, eigenfunctions
S	steady state
$*$	related to threshold value of K
$\pm$	at the boundaries $X=\pm1$

where $t_0=\rho cL^2/k$ and $\alpha=E_a/(k_BT_0^2)$, Eq. (1) and the boundary conditions become

$$\frac{\partial\theta}{\partial\tau}=\frac{\partial^2\theta}{\partial X^2}+\Lambda(X)e^{\theta} \tag{4}$$

$$\theta|_{X=-1}=\theta|_{X=+1}=0 \tag{5}$$

The dimensionless function $\Lambda(X)$ describes the way in which the structure of the packed bed is organized with respect to local intensity $Q_0(x)$ of the heat generation. In [1] it has been assumed that the structure exhibits a *plane-parallel stratification* described by the exponential law

$$\Lambda(X)=\lambda e^{sX} \tag{6}$$

Here λ and s are the *control parameters* of the problem. The *intensity parameter* λ is necessarily positive (exothermic reactions), while the *stratification parameter* s which characterizes the organized structure of the reacting material in the packed bed, may be positive, negative or zero. However, taking into account that the boundary value problem (4)–(6) is invariant under the transformations $(X\to-X, s\to-s)$, it is sufficient to consider only the non-negative values of the stratification parameter s, without any lost of generality.

The thermal evolution of the reactor is determined by the rate of heat generation by the exothermic reaction and the heat flux through the walls which are kept at the lower temperature T_0 (isothermal wall cooling). In the industrial practice one is interested to reach a time-independent (steady) working regime of the reactor in which between these two processes an exact balance holds. As it has been shown in [1], the dimensionless temperature field $\theta_S=\theta_S(X)$ of this *steady regime* is described by the exact analytical solution

$$\theta_S(X)=-\ln\left(\frac{e^{sX}}{K}\cosh^2\left[\sqrt{\frac{\lambda K}{2}}(X-X_0)\right]\right) \tag{7}$$

For determination of the two integration constants K and X_0 the boundary conditions furnish the relationships

$$\lambda=\frac{1}{2K}\left(\operatorname{arccosh}\sqrt{Ke^{s}}+\operatorname{arccosh}\sqrt{Ke^{-s}}\right)^2 \tag{8}$$

$$X_0=\frac{\operatorname{arccosh}\sqrt{Ke^{s}}-\operatorname{arccosh}\sqrt{Ke^{-s}}}{\operatorname{arccosh}\sqrt{Ke^{s}}+\operatorname{arccosh}\sqrt{Ke^{-s}}} \tag{9}$$

where $\operatorname{arccosh}(z)=\ln(z+\sqrt{z^2-1})$. The condition of existence of real solutions requires that for a given $s\geqslant0$, K is equal to, or larger than a threshold value $K_*=e^s$. The values of λ and X_0 corresponding to K_* are $\lambda_*=0$ and $X_0^*=0$ for $s=0$ and

$$\lambda_*=\frac{1}{2}e^{-s}\operatorname{arccosh}^2 e^{s} \quad\text{and}\quad X_0^*=1 \quad\text{for } s\neq0 \tag{10}$$

The basic features of the solution space can be inferred from the inspection of Fig. 1 where K has been plotted as a function of the intensity parameter λ for the value $s=1$ of the stratification parameter according to Eq. (8). The main message of Fig. 1 is that for a given value of the stratification parameter s, a maximum value $\lambda_{\max}(s)$ of the intensity parameter λ exists such that above of this *upper bound* no steady temperature solutions are possible. The domain of existence of the solutions is the finite λ-range $0<\lambda\leqslant\lambda_{\max}(s)$ for all $s\geqslant0$ and consists of a lower and an upper branch of the curve $K=K(\lambda)$, which match at the turning point $\lambda=\lambda_{\max}(s)$. The value $K=K_{\max}$ corresponding to $\lambda_{\max}(s)$ of λ is obtained as solution of the transcendental equation

$$\operatorname{arccosh}\sqrt{Ke^{s}}+\operatorname{arccosh}\sqrt{Ke^{-s}}=\sqrt{\frac{K}{K-e^{s}}}+\sqrt{\frac{K}{K-e^{-s}}} \tag{11}$$

and the maximum value $\lambda_{\max}(s)$ of the intensity parameter results as

$$\lambda_{\max}=\frac{K-\cosh s+\sqrt{K^2-2K\cosh s+1}}{K^2-2K\cosh s+1} \tag{12}$$

for $K=K_{\max}$.

In the range $0<\lambda<\lambda_*$ where λ_* is given by Eq. (10), the steady temperature solution (7) is always *unique*. In the range $\lambda_*\leqslant\lambda\leqslant\lambda_{\max}(s)$, however, dual lower- and upper-branch solutions occur which become coincident as $\lambda\to\lambda_{\max}(s)$. The lower branch

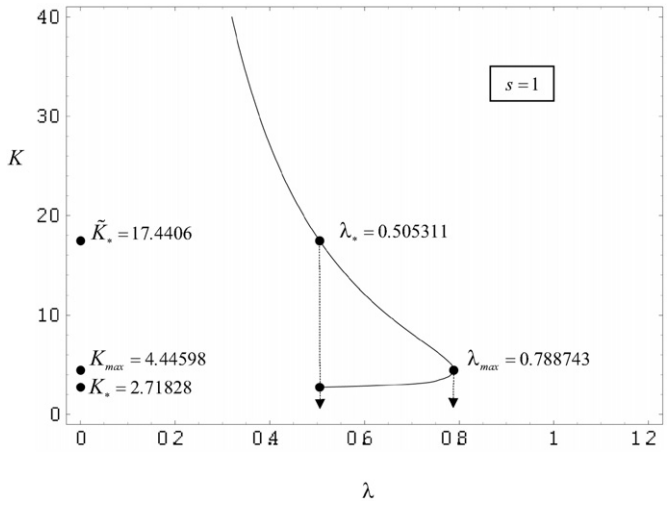

Fig. 1. Existence domain of the steady solutions (7) for $s = 1$. For given s, the intensity parameter λ is a univalued function $\lambda = \lambda(s; K)$ of the control parameter K in the whole range $K \geqslant K_* = e^s$.

solutions describe low-temperature and the upper branch solutions, high-temperature regimes of the exothermic reactions, respectively. Concerning the dual solutions, between the cases $s = 0$ (homogeneous reactor) and $s \neq 0$ (stratified reactor) an essential deviation is encountered. While in the case $s = 0$, the constant of integration X_0 is vanishing for all λ-values (which implies that for $s = 0$ all the dual solutions are symmetric with respect to the midplane $X = 0$ of the reactor), in the case $s \neq 0$ the dual solutions are always non-symmetric, being associated with different non-vanishing values of X_0. It is also worth noticing here that in the mathematical analysis of the problem, the quantity K (occurred initially as an integration constant) plays the role of an *order parameter* since, for a given s, the intensity parameter λ is a univalued function of K in its whole variation range $K \geqslant K_* = e^s$. The inverse function $K = K(\lambda)$, in contrast, possesses this property only for $0 < \lambda < \lambda_*$ and $\lambda = \lambda_{\max}$, but in the domain of existence $\lambda_* \leqslant \lambda < \lambda_{\max}(s)$ of the dual solutions, it is obviously bivalued (see Fig. 1).

3. Linearization and stability analysis

Every physical system is permanently exposed to infinitesimal perturbations coming from its environment. The perturbations generate in turn infinitesimal excitations of the system, which try to disintegrate its actual state. The internal dissipation forces of the system, on the other hand, try to prevent this decay by attenuating the excitations. In general, the result of this competition is either the restoration of the state of the system, or its definitive decay. The standard mathematical method to find out what in this respect in a given case actually happens is the *linear stability analysis*. The goal of the present section is to perform this analysis for the steady states (7) of the stratified reactor.

The first step is to linearize the full evolution equation (4) around the steady state (7) by the substitution

$$\theta(X, \tau) = \theta_S(X) + \varphi(X) e^{-\bar{\varepsilon}\tau} \tag{13}$$

where $\varphi(X)$ is the yet unknown infinitesimal excitation (*eigenstate*) of the system and $\bar{\varepsilon}$ is the corresponding *eigenvalue*. As a result of the linearization, one obtains the linear eigenvalue problem

$$\frac{d^2\varphi}{dX^2} + \left[\bar{\varepsilon} + \lambda e^{sX+\theta_S(X)}\right]\varphi = 0 \tag{14}$$

$$\varphi(-1) = \varphi(+1) = 0 \tag{15}$$

Eqs. (14) and (15) specify a Sturm–Liouville eigenvalue problem. From a more intuitive physical point of view, however, it is formally identical with a Schrödinger eigenvalue problem which describes the quantum mechanical motion of a particle in a one-dimensional box $X \in [-1, 1]$ with impenetrable boundaries at $X = \pm 1$. The latter feature results from the boundary conditions (15) along with the continuity requirement of the steady wave function $\varphi(X)$ at $X = \pm 1$, which outside of the box must vanish identically. The potential energy $V(X)$ of the particle in the box is

$$V(X) = -\lambda e^{sX+\theta_S(X)} = -\frac{\lambda K}{\cosh^2\left[\sqrt{\frac{\lambda K}{2}}(X - X_0)\right]} \tag{16}$$

It is interesting to notice that $-V(X)$ coincides precisely with rate of the local heat generation $Q_{\text{local}}(X)$ by the exothermic reaction (see Eqs. (32) and (33) of [1]).

Eq. (16) suggests that it is convenient to change from X to the new independent variable

$$\xi = \sqrt{\frac{\lambda K}{2}}(X - X_0) \tag{17}$$

Accordingly, the eigenvalue problem (14), (15) reduces to the simpler form

$$\frac{d^2\varphi}{d\xi^2} + \left(\varepsilon + \frac{2}{\cosh^2\xi}\right)\varphi = 0 \tag{18}$$

$$\varphi|_{\xi=\xi_-} = \varphi|_{\xi=\xi_+} = 0 \tag{19}$$

where $\varepsilon = 2\bar{\varepsilon}/(\lambda K)$, $\xi_- \leqslant \xi \leqslant \xi_+$ and

$$\xi_- = -\sqrt{\frac{\lambda K}{2}}(1 + X_0) = -\operatorname{arccosh}\sqrt{Ke^s}$$

$$\xi_+ = +\sqrt{\frac{\lambda K}{2}}(1 - X_0) = +\operatorname{arccosh}\sqrt{Ke^{-s}} \tag{20}$$

The main advantage of the quantum mechanical analogy described above consists of the fact that one can predict from the very beginning that the eigenvalue spectrum $\{\varepsilon\}$, i.e. the energy spectrum of the particle closed in the box, is purely discrete, non-degenerate, bounded from below and unbounded from above. Thus, ranking the eigenvalues ε_n according to their increasing values, $\varepsilon_0 < \varepsilon_1 < \varepsilon_2 < \cdots < \varepsilon_n < \cdots$, the corresponding eigenfunctions φ_n will automatically be ordered according to the increasing number of their zeros (*nodes*), such that φ_n has exactly n nodes, the *ground state* φ_0 being always nodeless (Sturm's *oscillation theorem*). These mathematical features are of basic importance for the linear stability analysis. Indeed, it is sufficient to determine whether (for a given s and K) the *energy* ε_0 of the (nodeless) ground state is positive or negative. When $\varepsilon_0 > 0$, all the other eigenvalues ε_n are also positive and the steady temperature distribution of the reactor $\theta_S(X)$ is stable against all the infinitesimal perturbations. All the excited states φ_n of $\theta_S(X)$ decay with time according to the exponential law $\exp(-\tilde{\varepsilon}_n\tau) = \exp(-\lambda K\varepsilon_n\tau/2)$ and the system returns to the unperturbed state $\theta_S(X)$ as $\tau \to \infty$. When however $\varepsilon_0 < 0$, then the perturbation φ_0 is amplified infinitely with time by the factor $\exp(|\tilde{\varepsilon}_0|\tau) = \exp(\lambda K|\varepsilon_0|\tau/2)$ as $\tau \to \infty$, which implies that initial steady state $\theta_S(X)$ is destroyed, i.e. the steady temperature field $\theta_S(X)$ is unstable against φ_0, as well as against all the other perturbations φ_n associated with negative eigenvalues ε_n. In this case, φ_0 represents the lowest instability mode of $\theta_S(X)$.

In addition to the positive and negative eigenvalues ε_n, the vanishing eigenvalue $\varepsilon_m = 0$, when exists, possesses a special significance for the stability analysis. In this case it is sufficient to determine whether the eigenfunction φ_m corresponding to $\varepsilon_m = 0$ is nodeless or not. Is φ_m nodeless, $\varepsilon_m = 0$ represents according to the oscillation theorem the lowest eigenvalue, i.e. $m = 0$. As a

consequence, the steady temperature field $\theta_S(X)$ in this case is *marginally* (or neutrally) stable against the perturbation φ_0 and stable against all the other perturbations φ_n, $n = 1, 2, 3, \ldots$. When, however, φ_m possesses at least one node, $\varepsilon_m = 0$ is not the lowest eigenvalue and the steady state $\theta_S(X)$ is unstable against all the perturbations φ_n with $n < m$.

Changing from ξ to the new independent variable z, $z = \tanh\xi$, Eq. (18) reduces to the differential equation of the Legendre functions of degree ν and order μ (see [11], Ch. 8),

$$(1-z^2)\frac{d^2\varphi}{dz^2} - 2z\frac{d\varphi}{dz} + \left[\nu(\nu+1) - \frac{\mu^2}{1-z^2}\right]\varphi = 0 \tag{21}$$

with $\nu = 1$ and

$$\mu = \sqrt{-\varepsilon} = i\sqrt{\varepsilon} \tag{22}$$

Thus, the *associated Legendre functions* of the first and second kind $P_\nu^\mu(z)$ and $Q_\nu^\mu(z)$ of degree $\nu = 1$ specify a system of *fundamental solutions* $\{\varphi_{\rm I}(\xi), \varphi_{\rm II}(\xi)\} = \{P_1^\mu(z), Q_1^\mu(z)\}$ of Eq. (21). Accordingly, the general solution of Eq. (18) is a linear combination of the fundamental solutions,

$$\varphi = C_{\rm I} P_1^\mu(\tanh\xi) + C_{\rm II} Q_1^\mu(\tanh\xi) \tag{23}$$

The boundary conditions (19) yield for the coefficients $C_{\rm I}$ and $C_{\rm II}$ the equations

$$\begin{aligned} &C_{\rm I} P_1^\mu(\tanh\xi_-) + C_{\rm II} Q_1^\mu(\tanh\xi_-) = 0 \\ &C_{\rm I} P_1^\mu(\tanh\xi_+) + C_{\rm II} Q_1^\mu(\tanh\xi_+) = 0 \end{aligned} \tag{24}$$

where, bearing in mind Eqs. (20),

$$\begin{aligned} \tanh\xi_- &= -\tanh\left(\operatorname{arccosh}\sqrt{Ke^s}\right) = -\sqrt{\frac{K-e^{-s}}{K}} \\ \tanh\xi_+ &= +\tanh\left(\operatorname{arccosh}\sqrt{Ke^{-s}}\right) = +\sqrt{\frac{K-e^{s}}{K}} \end{aligned} \tag{25}$$

The system of linear and homogeneous equations (24) admits nontrivial solutions for $C_{\rm I}$ and $C_{\rm II}$ only when its determinant is vanishing, i.e.,

$$\begin{aligned} Det \equiv\ & P_1^\mu(\tanh\xi_-) Q_1^\mu(\tanh\xi_+) \\ & - P_1^\mu(\tanh\xi_+) Q_1^\mu(\tanh\xi_-) = 0 \end{aligned} \tag{26}$$

For given values of s and K, the roots of Eq. (26) determine the eigenvalue spectrum $\varepsilon_0 < \varepsilon_1 < \varepsilon_2 < \cdots$ of the problem. Since the differential equation (18), as well as the boundary conditions (19) are linear and homogeneous, the eigenfunctions (23) corresponding to the eigenvalues ε_n are determined only to a constant factor. Accordingly, they can be normalized to our convenience. With the aim of a simple comparison with the direct numerical solution of the eigenvalue problem (18), (19) (see Section 4), we require that at the left boundary $\xi = \xi_-$ of the reactor the slope of the normalized eigenfunctions $\bar\varphi$ equals unity, i.e. $(d\bar\varphi/d\xi)|_{\xi=\xi_-} = 1$. Therefore, our eigenfunctions normalized in this way will be obtained as

$$\bar\varphi = \frac{\varphi}{(d\varphi/d\xi)|_{\xi=\xi_-}} \tag{27}$$

where φ is specified by Eqs. (23)–(26). After some algebra one gets

$$\bar\varphi = \frac{Q_1^\mu(\tanh\xi_-) P_1^\mu(\tanh\xi) - P_1^\mu(\tanh\xi_-) Q_1^\mu(\tanh\xi)}{Q_1^\mu(\tanh\xi_-)\frac{dP_1^\mu(\tanh\xi)}{d\xi}\big|_{\xi=\xi_-} - P_1^\mu(\tanh\xi_-)\frac{dQ_1^\mu(\tanh\xi)}{d\xi}\big|_{\xi=\xi_-}} \tag{28}$$

Now we turn to the detailed discussion of the eigenvalue problem (18), (19). The eigenvalue spectrum is obtained as roots ε of Eq. (26) for specified K and s. This equation is real for $\varepsilon \leqslant 0$ but becomes complex in the range $\varepsilon > 0$. Thus the roots ε of $Det = 0$ are the simultaneous zeros of Re[*Det*] and Im[*Det*], i.e. the zeros of $|Det|$. As a first illustration of the distribution of eigenvalues $\varepsilon_0 < \varepsilon_1 < \varepsilon_2 < \cdots$, in Fig. 2 the expression of $|Det|$ has been plotted as a function of ε for $s = 1$ and $K = K_* = e^s$. The roots $\varepsilon_0 < \varepsilon_1 < \varepsilon_2 < \cdots$ of $Det = 0$ are given by the contact points of the curve $|Det|$ with the ε-axis. One sees, that in this case all the eigenvalues are positive. Accordingly, the steady temperature distribution (7) corresponding to $s = 1$ and to the threshold value $K_* = e^s$ of K is linearly stable.

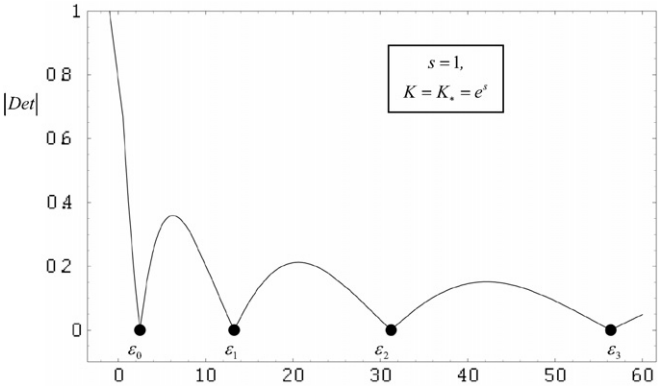

Fig. 2. The eigenvalues $\varepsilon_0 < \varepsilon_1 < \varepsilon_2 < \cdots$ correspond to the contact points (dots) of the curve $|Det|$ with the $\tilde\varepsilon$-axis. In the present case $\varepsilon_0 = 2.47554$, $\varepsilon_1 = 13.2493$, $\varepsilon_2 = 31.2122$, $\varepsilon_3 = 56.3607, \ldots$.

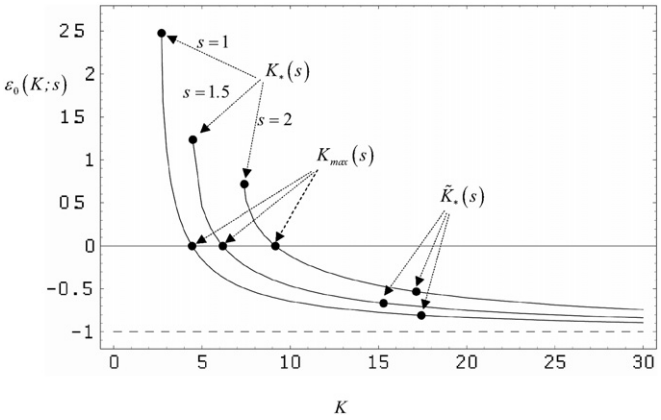

Fig. 3. The lowest eigenvalue $\varepsilon_0(K;s)$ is a monotonically decreasing function of K for in the whole range $K \geqslant K_* = e^s$ for $s = 1$, 1.5 and 2. The dots in the upper half plane mark the largest value of $\varepsilon_0(K;s)$ corresponding to the respective threshold values $K_*(s) = e^s$ of K, whereas those in the lower half plane correspond to the dual counterparts $\tilde K_*(s)$ of $K_*(s)$ associated with the same values $\lambda_*(s)$ of λ (see Fig. 1). The intersection points of the curves $\varepsilon_0(K;s)$ with the K-axis correspond precisely to the values $K_{\max}$ associated with the maximum value $\lambda_{\max}(s)$ of the intensity parameter. In the range $K > K_{\max}$ the lowest eigenvalue is negative and approaches -1 as $K \to \infty$ (dashed line).

As explained above, we are basically interested in the position-change of the lowest eigenvalue ε_0 with increasing values of K in the whole range $K \geqslant K_* = e^s$ for given values of the stratification parameter s. To be specific, in Fig. 3 the dependence of the lowest eigenvalue ε_0 on K has been plotted for three different values $s = 1$, 1.5 and 2 of the stratification parameter in the corresponding ranges $K \geqslant K_* = e^s$ of K (see also Fig. 1). One sees that the lowest eigenvalue $\varepsilon_0(K;s)$ always is a monotonically decreasing function of K for in the whole range $K \geqslant K_* = e^s$ for $s = 1$, 1.5 and 2. The dots in the upper half plane mark the largest values of $\varepsilon_0(K;s)$ corresponding to the respective threshold values $K_*(s) = e^s$ of K, whereas those in the lower half plane correspond to the dual counterparts $\tilde K_*(s)$ of $K_*(s)$, associated with the same values $\lambda_*(s)$ of λ (see Fig. 1, and Table 1 of [1]). The intersection points of the

curves $\varepsilon_0(K;s)$ with the K-axis correspond precisely to the values $K_{\max}(s)$ associated with the maximum value $\lambda_{\max}(s)$ of the intensity parameter (see also Table 1 of [1]). In the range $K > K_{\max}$, the lowest eigenvalue is negative and approaches -1 as $K \to \infty$. The above features hold for all $s \geqslant 0$. One arrives in this way to the important conclusion that the lower branch (low-temperature) solutions are always linearly stable, while the upper branch ones (high-temperature solutions) linearly unstable. The steady state of the reactor corresponding to the matching point $\lambda = \lambda_{\max}(s)$ of the low- and high-temperature solutions is marginally stable since the lowest eigenvalue in this point is vanishing, $\varepsilon_0(K_{\max};s) = 0$ for all $s \geqslant 0$. In other words, the *unique* upper branch solutions associated with K-values in the range $K > \tilde{K}_*(s)$ are all unstable. The lower branch solutions in the K-range $K_*(s) \leqslant K < K_{\max}(s)$ are always linearly stable, but their *dual* upper branch counterparts with $K_{\max}(s) < K \leqslant K_*(s)$ are unstable. The stable and unstable solution branches are joined at $K = K_{\max}(s)$ by a marginally stable unique solution.

The feature $\varepsilon_0(K_{\max};s) = 0$ for all $s \geqslant 0$, can also be proven analytically. Indeed, taking into account that for $\mu = 0$ (i.e. $\varepsilon = 0$) the associated Legendre functions have the simple expressions

$$P_1^0(\tanh\xi) = \tanh\xi,$$
$$Q_1^0(\tanh\xi) = -1 + \xi\tanh\xi \tag{29}$$

the eigenvalue equation (26) becomes

$$\xi_+ - \xi_- = \frac{1}{\tanh\xi_+} - \frac{1}{\tanh\xi_-} \tag{30}$$

Bearing in mind Eqs. (20) and (25), it is easy to see that Eq. (29) coincides exactly with Eq. (11) which determines the value $K = K_{\max}$ corresponding to the maximum $\lambda_{\max}(s)$ of the intensity parameter λ. Therefore, in the state of the reactor corresponding (for a given s) to the maximum of the of the intensity parameter, $\varepsilon = 0$ is surely an eigenvalue. Hence, with respect to the stability of the steady state corresponding to $\lambda_{\max}(s)$, the key question is whether in this case $\varepsilon = 0$ is the lowest eigenvalue or not. The answer on this question is obtained from the corresponding eigenmode (28) which in the present case reads

$$\begin{aligned}\bar{\varphi} &= (1-\xi_-\tanh\xi_-)\tanh\xi - (\tanh\xi_-)(1-\xi\tanh\xi)\\ &= \left(1 - \sqrt{\frac{K_{\max}-e^{-s}}{K_{\max}}}\,\operatorname{arccosh}\sqrt{K_{\max}e^{s}}\right)\tanh\xi\\ &\quad + \sqrt{\frac{K_{\max}-e^{-s}}{K_{\max}}}(1-\xi\tanh\xi)\end{aligned} \tag{31}$$

In Fig. 4 the eigenmode (31) is plotted as a function of $\xi \in [\xi_-, \xi_+]$ for four selected values of $s, s = 0, 1, 1.5$ and 2, where the corresponding solutions of Eq. (11) are $K_{\max} = 3.27672$, 4.44598, 6.17899 and 9.17882, respectively (see also Table 1 of [1]). It is seen that the eigenfunction (31) is nodeless for all values of the stratification parameter s, which means that $\varepsilon = 0$ is the lowest eigenvalue for all s when $\lambda = \lambda_{\max}(s)$. Hence, these eigenfunctions describe the marginally stable modes of the steady temperature distribution $\theta_S(X)$ corresponding to $\lambda = \lambda_{\max}(s)$. We may further conclude that the eigenvalues $\varepsilon_1 < \varepsilon_2 < \varepsilon_3 < \cdots$ larger than $\varepsilon_0 = 0$ are associated with stable modes $\bar{\varphi}_n$, $n = 1, 2, 3, \ldots$, of the temperature distribution $\theta_S(X)$ corresponding to $\lambda = \lambda_{\max}(s)$. To be specific, in Fig. 5 the normalized eigenfunctions (28) corresponding to $\varepsilon_0, \varepsilon_1, \varepsilon_2$ and ε_3 are shown for the case ($s = 1, K = K_{\max} = 4.44598$), where $\varepsilon_0 = 0, \varepsilon_1 = 4.41955, \varepsilon_2 = 11.4648, \varepsilon_3 = 21.3183, \ldots$. One clearly sees that the number of nodes of the eigenfunctions $\bar{\varphi}_n$ equals n, in full agreement with the oscillation theorem.

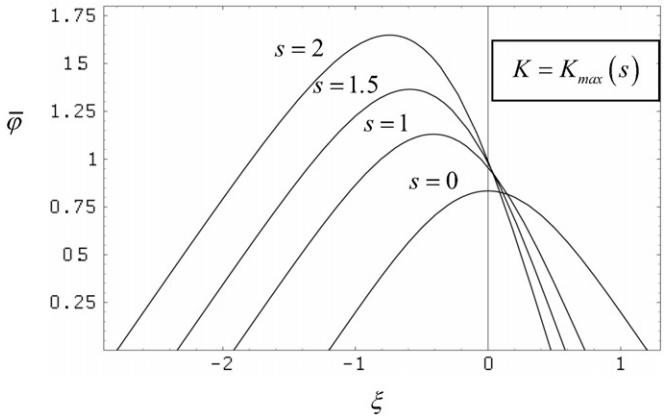

Fig. 4. Plotted are the eigenfunctions (31) associated with the matching point $\{K, \lambda\} = \{K_{\max}(s), \lambda_{\max}(s)\}$ of the lower- and upper-branch solutions for $s = 0, 1, 1.5$ and 2, respectively. The corresponding eigenvalues being vanishing, $\varepsilon = 0$, the functions $\bar{\varphi}$ describe the marginally stable modes of the steady temperature distributions $\theta_S(X)$ corresponding to $\{K, \lambda\} = \{K_{\max}(s), \lambda_{\max}(s)\}$.

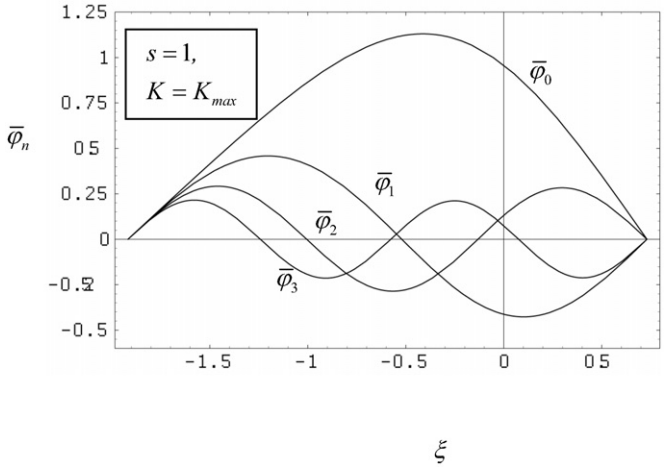

Fig. 5. The first four eigenmodes of the steady temperature profile $\theta_S(X)$ corresponding to the matching point $\{K, \lambda\} = \{K_{\max}(s), \lambda_{\max}(s)\}$ of the lower- and upper-branch solutions for $s = 1$. The temperature distribution $\theta_S(X)$ is marginally stable with respect to the mode $\bar{\varphi}_0$ corresponding to the lowest eigenvalue $\varepsilon_0 = 0$, and stable with respect to $\bar{\varphi}_n$, $n = 1, 2, 3, \ldots$.

4. Numerical validation

The aim of the present section is to confirm the analytical results of Section 3 by a direct numerical solving of the eigenvalue problem (18), (19). The numerical approach can be simplified substantially by exploiting the fact that both Eq. (18) and the boundary conditions (19) are linear and homogeneous. Indeed, these features allow one to formally reduce the *eigenvalue problem* (18), (19) to *the initial value problem*

$$\frac{d^2\varphi}{d\xi^2} + \left(\varepsilon + \frac{2}{\cosh^2\xi}\right)\varphi = 0$$
$$\varphi|_{\xi=\xi_-} = 0, \qquad \left.\frac{d\varphi}{d\xi}\right|_{\xi=\xi_-} = 1 \tag{32}$$

subject to the additional forcing condition

$$\varphi|_{\xi=\xi_+} = 0 \tag{33}$$

The first initial condition (32) coincides with the first boundary condition (19), while the second one is the requirement that the "*initial velocity*" (i.e. slope of the eigenfunctions at the left boundary $\xi = \xi_-$) always equals 1. Owing to the linear and homogeneous

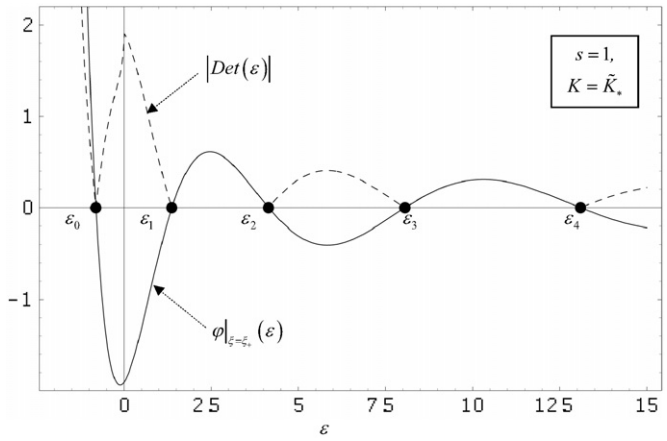

Fig. 6. The solid curve $\varphi|_{\xi=\xi_+}(\varepsilon)$ is obtained from the direct numerical solution of the eigenvalue problem and the dashed curve $|Det(\varepsilon)|$ represents the left hand side of the eigenvalue equation (26) for $s=1$ and $K=\tilde{K}_*=17.4406$. The coincident intersection points of the two curves with the ε-axis (dots) yield the eigenvalue spectrum $\varepsilon_0<\varepsilon_1<\varepsilon_2<\cdots$, where $\varepsilon_0=-0.80781$, $\varepsilon_1=1.37133$, $\varepsilon_2=4.14609$, $\varepsilon_3=8.05852,\ldots$. In the ranges $[\varepsilon_1,\varepsilon_2],[\varepsilon_3,\varepsilon_4],\ldots$ the two curves are overlapping.

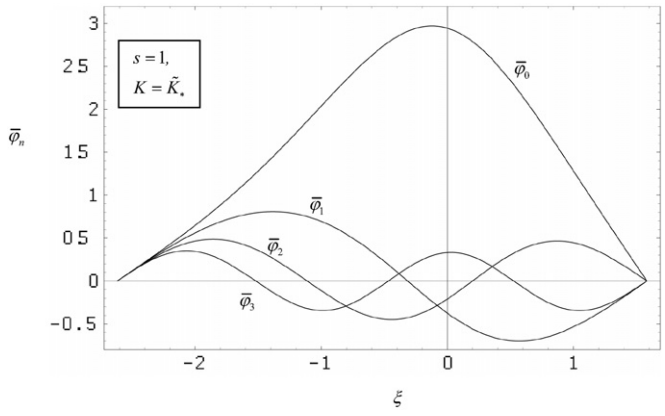

Fig. 7. The first four eigenmodes of the upper branch temperature profile $\theta_S(X)$ corresponding to the point $(\lambda,K)=(\lambda_*,\tilde{K}_*)=(0.505311,17.4406)$ of Fig. 1. The lowest eigenvalue being negative, $\varepsilon_0=-0.80781$, $\bar{\varphi}_0$ represents the instability mode of this $\theta_S(X)$. The plots of the numerical and the corresponding analytical solutions (28) are full overlapping.

character of the eigenvalue problem, this latter condition may be imposed without any restriction of generality. In this way, using the numerical solution of the initial value problem (32), it is sufficient to plot $\varphi|_{\xi=\xi_+}$ (which represents the "position" φ at the final instant $\xi=\xi_+$ of motion) as a continuous function of the eigenvalue parameter ε. The zeros of this curve $\varphi|_{\xi=\xi_+}=\varphi|_{\xi=\xi_+}(\varepsilon)$ are precisely the ε-values for which the additional condition (33) is satisfied, i.e., the eigenvalues $\varepsilon_0<\varepsilon_1<\varepsilon_2<\cdots$ which we are interested in. As an illustration, in Fig. 6 the curve $\varphi|_{\xi=\xi_+}(\varepsilon)$ obtained in this way is compared to the curve $|Det(\varepsilon)|$ based on Eq. (26) for $s=1$ and $K=\tilde{K}_*=17.4406$ which, according to Fig. 1, represents the dual upper branch counterpart of the lower branch point $K=K_*=2.71828$, both being associated with the same value $\lambda=\lambda_*=0.505311$ of the intensity parameter. From Fig. 6, two main messages can be inferred, namely (i) the eigenvalues obtained by analytical calculations as roots of equation $|Det(\varepsilon)|=0$ on the one hand, and by a direct numerical solution of the eigenvalue problem as roots of equation $\varphi|_{\xi=\xi_+}(\varepsilon)=0$ on the other hand, coincide exactly, (ii) the lowest eigenvalue $\varepsilon_0=-0.80781$ is negative, i.e. the upper branch (high-temperature) solution $\theta_S(X)$ associated with $(\lambda,K)=(\lambda_*,\tilde{K}_*)=(0.505311,17.4406)$ and $s=1$ is unstable, in full agreement with Fig. 3. The instability mode $\bar{\varphi}_0$ of this $\theta_S(X)$ as well as its stable excited states $\bar{\varphi}_n$ corresponding to the eigenvalues $\varepsilon_1=1.37133$, $\varepsilon_2=4.14609$ and $\varepsilon_3=8.05852$ are plotted in Fig. 7. Similarly to Fig. 5, the validity of the oscillation theorem is clearly seen also in this case.

5. Summary and conclusions

The linear stability of steady conduction regime of a parallel-plane packed bed reactor with a stratified structure and internal volumetric heat generation by exothermic reactions has been investigated. The approach was based on an exactly solvable one-dimensional nonlinear mathematical model which involves two experimentally accessible control parameters, the intensity parameter λ and stratification parameter s. From engineering point of view, this model corresponds to a three-dimensional reactor whose y- and z-dimensions are much larger than the x-dimension, i.e. than the distance $2L$ between the two plane boundaries (Fig. 1). In this case the finite-size effects in y- and z-directions of the real reactor can be neglected, and the results of the (mathematically) one-dimensional model calculations hold in the three-dimensional world as well. The intensity parameter λ is an intrinsic material constant which is determined by the reaction heat. The stratification parameter s is rather a geometrical characteristic which is determined by the way in which the structure of the reacting materials has been organized between the plane boundaries. For a given value of s, an upper bound $\lambda_{\max}(s)$ of λ exists, such that above of this maximum no steady state solutions are possible. Below $\lambda_{\max}(s)$, unique as well as dual solutions exist. The former ones describe high temperature steady states of the reactor, while the dual solution branches are associated with low and high temperature reaction regimes, respectively. The main results of the stability analysis of these steady temperature distributions can be summarized as follows.

1. The basic eigenvalue problem of the stability analysis coincides formally with a *Schrödinger eigenvalue problem* of a particle in a one-dimensional box with impermeable walls. The negative potential energy of the particle $-V(X)$ coincides with rate of the local heat generation $Q_{\text{local}}(X)$ by the exothermic reaction. Thus, the eigenvalue spectrum is completely discrete, non-degenerate, bounded from below and unbounded from above. Ranking the eigenvalues ε_n according to their increasing values $\varepsilon_0<\varepsilon_1<\varepsilon_2<\cdots<\varepsilon_n<\cdots$, the corresponding eigenfunctions φ_n will automatically be ordered according to the increasing number of their zeros (*nodes*), such that φ_n has exactly n nodes, the *ground state* φ_0 being always nodeless (Sturm's *oscillation theorem*).
2. The eigenfunctions φ_n can be given in exact analytical form as linear combinations of the associated Legendre functions of the first and second kind.
3. The lowest eigenvalue $\varepsilon_0=\varepsilon_0(s;K)$ is for all $s\geqslant 0$ a monotonically decreasing function of the *order parameter* K in the whole domain of existence $K\geqslant e^s\equiv K_*(s)$ of the steady temperature solutions $\theta_S(X)$ (see Fig. 3).
4. The lowest eigenvalue $\varepsilon_0=\varepsilon_0(s;K)$, and thus the whole spectrum, is positive for all $e^s\equiv K_*(s)\leqslant K<K_{\max}(s)$ and $s\geqslant 0$, i.e. for all the possible low-temperature distributions $\theta_S(X)$ of the reactor. In this range all the linear excitations φ_n of $\theta_S(X)$ decay exponentially with time. Accordingly, *all the lower-branch solution,* $0<\lambda<\lambda_{\max}(s)$, *are linearly stable*.
5. At $K_{\max}(s)$, i.e. at the K-value corresponding to $\lambda=\lambda_{\max}(s)$, the lowest eigenvalue becomes zero, $\varepsilon_0(s;K_{\max})=0$. Consequently, the temperature distribution $\theta_S(X)$ corresponding to the maximum value $\lambda_{\max}(s)$ of the intensity parameter is *marginally stable* for all $s\geqslant 0$.

6. As K exceeds the value $K_{\max}(s)$, the lowest eigenvalue $\varepsilon_0 = \varepsilon_0(s;K)$ changes its sign from plus to minus (see Fig. 3). Accordingly, $\lambda = \lambda_{\max}(s)$ marks at the same time that point of the parameter plane where the reactor changes from a linearly stable to an unstable steady regime. All the upper branch (i.e. high temperature) steady states, both in the range $K_{\max} < K \leqslant \tilde{K}_*$ of the dual solutions and in the range $K > \tilde{K}_*$ of the unique solutions as well (see Fig. 1), are *unstable*.
7. As physically expected, the upper bound $\lambda = \lambda_{\max}(s)$ of the existence domain of the steady regime decreases with increasing value of the stratification parameter s. In other words, $\lambda = \lambda_{\max}(0)$ corresponding to the homogeneous reactor, represents the absolute upper limit of stability of the low temperature solutions for all $s \geqslant 0$.

References

[1] E. Magyari, Steady thermal regimes of a parallel-plane packed bed reactor with an organized structure, Chem. Eng. J. 146 (2009) 136–142.
[2] E.J. Westernik, N. Koster, K.R. Westerterp, The choice between cooled tubular reactor models: Analysis of the hot spot, Chem. Eng. Sci. 45 (1990) 3443–3455.
[3] C.-H. Li, B.A. Finlayson, Heat transfer in Packed bed. A reevaluation, Chem. Eng. Sci. 32 (1977) 1055–1066.
[4] J.H.T. Luong, B. Volesky, A new technique for continuous measurement of heat of fermentation, Eur. J. Appl. Microbiol. Biotechnol. 16 (1982) 28–34.
[5] F.-J. Ulm, O. Coussy, Strength growth as. chemo-plastic hardening in early age concrete, ASCE J. Eng. Mech. 122 (1996) 1123–1132.
[6] G. DeSchutter, Fundamental study of early-age concrete behavior as a basis for durable concrete structures, Materials and Structures 35 (2002) 15–21.
[7] C.V. Nielson, A. Berrig, Temperature calculations during hardening, Concrete Internat. 27 (2005) 73–76.
[8] P. Frantzis, Effect of early-age temperature rise on stability of rapid-hardening cement fiber composites, ASCE J. Mater. Civil Eng. 18 (2006) 568–575.
[9] P. Gray, P.R. Lee, Thermal explosion theory, Oxidation and Combustion Reviews 2 (1967) 3–183.
[10] D.A. Frank-Kamenetskii, Diffusion and Heat Exchange in Chemical Kinetics, Plenum Press, New York, 1969.
[11] M. Abramowitz, I.A. Stegun, Handbook of Mathematical Functions, Dover, New York, 1970.